Available online at www.sciencedirect.com
SCIENCE DIRECT®
Chemical Physics Letters 381 (2003) 479–485
CHEMICAL PHYSICS LETTERS
www.elsevier.com/locate/cplett

An experimental manifestation of distinct electronic–structural properties of covalent dimer anions of CO_2 and CS_2

Richard Mabbs, Eric Surber, Andrei Sanov *

Department of Chemistry, University of Arizona, Tucson, AZ 85721-0041, USA

Received 30 July 2003
Published online: 24 October 2003

Abstract

Photoelectron imaging is employed to examine the monomer and dimer anions of CO_2 and CS_2, either isolated or embedded in clusters. In both cases, photodetachment from the dimer anion is compared to the corresponding monomer. The comparison of CS_2^- and $(CS_2)_2^-$ images reveals dissimilar bands attributed to detachment from different orbitals/species. Yet the photoelectron angular distributions obtained from the monomer and dimer anion cores of $(CO_2)_n^-$ clusters are surprisingly similar. These findings are reconciled with the qualitatively different electronic–structural properties of $(CS_2)_2^-$ and $(CO_2)_2^-$.

1. Introduction

Recent years have seen an explosion of interest in the imaging [1] approach to photoelectron spectroscopy [2] as a technique of choice for probing the structure and dynamics of neutral and ionic species [3]. Of particular importance is the relative ease of determination of the photoelectron angular distributions (PADs), along with the energy-resolved spectra. These coupled observables are viewed as signatures of the bound electron orbitals and electron emission mechanisms [4].

Since the properties of molecular cluster anions are largely determined by their ionic cores [5–12], photoelectron imaging, specifically targeting the electronic structure, is helpful in characterizing these intriguing species [13–15]. In this work, photoelectron imaging is used to examine the monomer and dimer anions of CO_2 and CS_2, either isolated or embedded in clusters. We focus on these members of the isovalent CO_2/OCS/CS_2 family, because the structures of the corresponding dimer anions show the most prominent contrast.

Calculations predict that the $(CO_2)_2^-$, $(OCS)_2^-$, and $(CS_2)_2^-$ global potential minima correspond to covalent structures with the excess electron shared between two monomer groups [6,12,16–18]. However, under certain solvation conditions monomer-based clusters may become more favorable. For

* Corresponding author.
E-mail address: sanov@u.arizona.edu (A. Sanov).

0009-2614/$ - see front matter © 2003 Elsevier B.V. All rights reserved.
doi:10.1016/j.cplett.2003.09.146

example, while $(CO_2)_n^-$, $2 \leqslant n < 6$ have dimer-anion cores, only CO_2^- based species are observed in the $n = 7$–13 range [11,19]. For $(CS_2)_n^-$, the monomer and dimer based clusters coexist for $n = 2$–6 [15,18], with a similar trend in $(OCS)_n^-$ [14].

Considering the dimer anion properties, it is revealing that the most stable $(CO_2)_2^-$ structure has D_{2d} symmetry and a relatively weak C–C bond [16], yet the corresponding dimer anions of OCS and CS_2 have more tightly bound, cyclic C_{2v} structures with C–C and S–S bonds [6,12]. More importantly, the two types of dimer anions differ in their electron configurations. In $(CO_2)_2^-$ the excess electron occupies an orbital which diabatically corresponds to the LUMO of a neutral (van der Waals) dimer. To the contrary, the excess electron in $(CS_2)_2^-$ or $(OCS)_2^-$ occupies an orbital of a different nature. Jordan and co-workers argued [12,17] that the electron configurations of these anions arise from the addition of an electron to the doubly excited neutral configurations, which themselves result from singlet coupling of two neutral monomers excited to their respective triplet states. The relatively large singlet-triplet splitting in CO_2 makes the cyclic dimer anion structure energetically unfavorable compared to the van der Waals-based D_{2d} structure, while in $(OCS)_2^-$ and $(CS_2)_2^-$ the cyclic C_{2v} structures prevail.

Photoelectron imaging can reveal differences in the electronic symmetry of the species studied. In this work, we compare the detachment from the monomer and dimer orbitals of the CO_2 and CS_2 based species and observe clear evidence of the fundamentally different electronic structures of covalent $(CO_2)_2^-$ and $(CS_2)_2^-$.

2. Experimental apparatus

The apparatus is described in detail elsewhere [20]. It employs the techniques of pulsed ion spectroscopy [21], combined with the velocity-map [22] photoelectron imaging detection.

The ions are formed in an electron-impact ionised, pulsed supersonic expansion and extracted into a time-of-flight mass-spectrometer. The ion beam is then crossed with the beam from an amplified Ti:Sapphire laser system (Spectra Physics). A portion of the 800 nm fundamental output is frequency-doubled to give 400 nm, 120 μJ pulses. The laser beam is mildly focussed using a 2 m focal length lens positioned 1.3 m before the crossing with the ion beam.

The photoelectrons are detected in the direction perpendicular to the ion and laser beams using a 40 mm diameter microchannel-plate detector with a phosphor screen (Burle, Inc.) mounted at the end of a shielded electron flight tube. All images contain the axis of cylindrical symmetry (z) defined by the linear polarization of the laser beam. This allows for the three-dimensional photoelectron velocity/angular distributions to be reconstructed using the Abel-transform method in the implementation of Reisler and co-workers [23].

3. Results

Fig. 1 presents 400 nm photoelectron images obtained from CS_2^- and $(CS_2)_2^-$. Both raw and Abel-transformed data are shown. The CS_2^- image

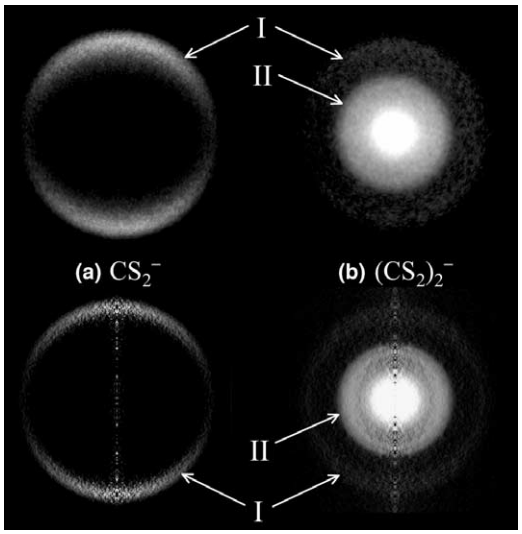

Fig. 1. 400 nm photoelectron images of (a) CS_2^- and (b) $(CS_2)_2^-$. The raw and Abel-transformed images are shown in the top and bottom parts of the Figure, respectively. The laser polarization is vertical. Arrows I point to the transitions corresponding to electron detachment from the CS_2^- HOMO (either in the isolated anion or in the $CS_2^- \cdot CS_2$ cluster). Arrow II marks the lowest-energy detachment transition from covalent $(CS_2)_2^-$.

contains a single band (I) corresponding to a vertical detachment energy (VDE) of 1.43 eV, in agreement with the previously published CS_2^- photoelectron spectra [10,18,24–26]. The PAD is described by an anisotropy parameter $\beta = 0.60$, consistent with electron ejection from the a_1 HOMO of CS_2^- [20,26].

The $(CS_2)_2^-$ image in Fig. 1b reveals several transitions. The weak outer band (I) has the energetics (VDE = 1.65 eV) and anisotropy ($\beta = 0.34$) consistent with the HOMO detachment from CS_2^- solvated by neutral CS_2. None of the other bands in the image are attributable to the $CS_2^- \cdot CS_2$ structure. The isotropic spot at the center is due mainly to autodetachment from either the excited state(s) of covalent $(CS_2)_2^-$ or its photofragments [15]. Ring II is assigned to the lowest-energy detachment transition in covalent $(CS_2)_2^-$, corresponding to VDE ≈ 2.7 eV and $\beta = -0.17$. The different properties of the transitions involving the covalent dimer anion HOMO (band II in Fig. 1b) and the HOMO of CS_2^- (band I in Figs. 1a and b) are of particular interest to this work. The opposite signs of the anisotropy are consistent with the contrasting natures of the monomer and dimer anion orbitals. As expected, *detachment from different orbitals* (belonging to different species) *yields distinctly different bands in the photoelectron images*.

The $(CO_2)_n^-$, $n = 4$–9 images are shown in Fig. 2. We emphasize the similarities between all n: only one broad transition is apparent and the PADs always peak along the laser polarization axis. In particular, these results quantify the observation noted in passing by Johnson and co-workers [11] that all of the negatively charged CO_2 clusters studied displayed strong, positive photoelectron anisotropies. The similarity of the images is rather striking in view of $(CO_2)_n^-$ core-switching [11,19], which can be seen in Fig. 2. Note the larger size of the $n = 6$ and 7 images compared to $n = 5$ (all images were recorded with the same electron lens voltages). The presence of faster electrons suggests a lower VDE for the larger-size clusters, which is the effect that led Johnson and co-workers to discover that $(CO_2)_n^-$, $2 \leqslant n < 6$ have dimer-anion cores, the $7 \leqslant n \leqslant 13$ clusters are monomer based, while both types coexist for $n = 6$ [11].

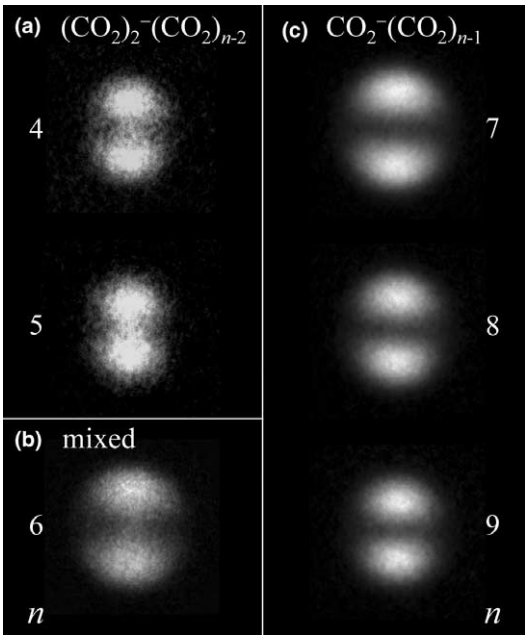

Fig. 2. 400 nm photoelectron images of $(CO_2)_n^-$, $n = 4$–9 cluster anions. The laser polarization is vertical. (a) Images for $n = 4$ and 5 corresponding to the dimer-based cluster anions $(CO_2)_2^-(CO_2)_{n-2}$. (b) $(CO_2)_6^-$ image corresponding to coexisting $(CO_2)_2^-(CO_2)_4$ and $CO_2^-(CO_2)_5$ cluster anions. (c) Images for $n = 7$–9 corresponding to the monomer-based cluster anions $CO_2^-(CO_2)_{n-1}$.

Fig. 3 shows the variations in photoelectron anisotropy with energy for representative monomer and dimer based $(CO_2)_n^-$. In all cases, β is contained within the same narrow range. Thus, for $(CO_2)_n^-$ *the detachment from the monomer and dimer anion HOMOs yields qualitatively similar photoelectron bands*. This result may seem counterintuitive and it also contrasts the observations for CS_2^- and $(CS_2)_2^-$. In the next Section it will be reconciled with the known monomer and dimer anion properties.

4. Discussion

The most intriguing result of this study is the similarity of the PADs obtained from the monomer and dimer based $(CO_2)_n^-$. Given the different types of cluster cores and bound orbitals from which the electrons are ejected, one expects these

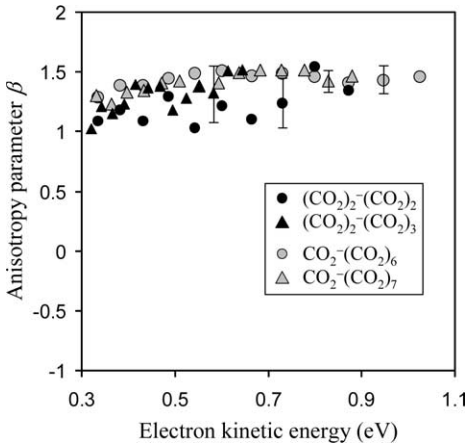

Fig. 3. Energy dependence of the photoelectron anisotropy for representative monomer-based (gray symbols) and dimer-based (black symbols) $(CO_2)_n^-$ cluster anions (derived from the data in Fig. 2). The error bars reflect one standard deviation in the data.

differences to be reflected in the PADs, contrary to the experimental indications. An even more intriguing perspective is derived from the comparison with CS_2^- and $(CS_2)_2^-$, which do indeed yield strikingly different PADs. The discrepancy between the CS_2 and CO_2 based systems reflects fundamental differences in the corresponding dimer anions. We begin by examining the $(CO_2)_2^-$ HOMO and adapt the previously described s and p model of photodetachment [20] to the comparative treatment of CO_2^- and covalent $(CO_2)_2^-$.

In this model, the molecular frame (MF) to laboratory frame (LF) transformation and orientation averaging are accounted for qualitatively by including only few 'principal' orientations of the anion. Principal orientations correspond to one transition dipole moment component aligned along the laser polarization axis (z). The arrangement of the HOMO for two such orientations of $(CO_2)_2^-$ is shown in Fig. 4. The structure of covalent $(CO_2)_2^-$ belongs to the D_{2d} point group [16] and its HOMO corresponds to the A_1 irreducible representation (i.r.). Orientations I and II correspond to the E and B_2 representations, respectively, of the laser electric-field vector in the dimer MF.

The $(CO_2)_2^-$ HOMO (ψ_{dimer}) can be thought of as a superposition of two monomer orbitals and hence the detachment from it can be described in

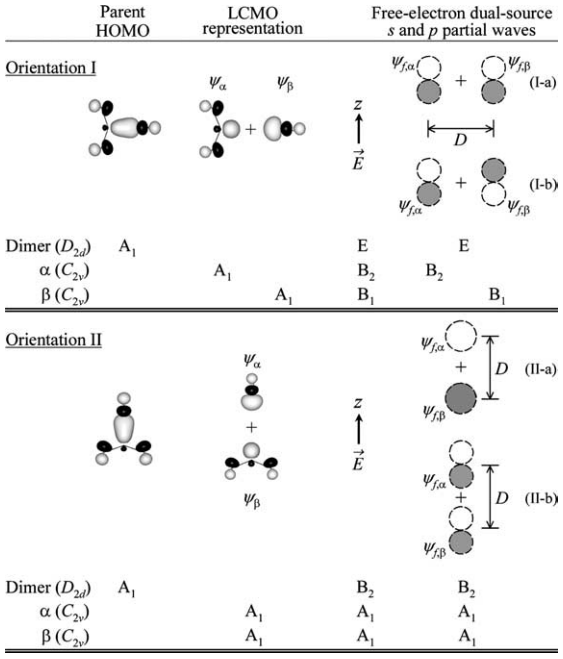

Fig. 4. Qualitative treatment of $(CO_2)_2^-$ photodetachment. For each orientation I and II, the parent orbital (left column) is described as an LCMO superposition of the orbitals of two monomers α and β (second column). The partial wave pairs sketched on the right represent a dual-source description of the free-electron wavefunction in the limit of s and p components only. The symmetries of the bound and free electron wavefunctions and the laser polarization vector are given in the irreducible representations of the dimer and monomer point groups (D_{2d} and C_{2v}, respectively).

terms of interference of electron waves originating from the two CO_2 moieties in the dimer anion. This correlation will enable us to compare the $(CO_2)_2^-$ and CO_2^- PADs. Using a Linear Combination of Molecular Orbitals (LCMO) approach and disregarding the normalization, we assume:

$$\psi_{\text{dimer}} \approx \psi_\alpha + \psi_\beta, \tag{1}$$

where $\psi_{\alpha,\beta}$ are the HOMOs of two (hypothetical) monomer anions (α and β) separated by the C–C bond (see Fig. 4). The monomer units and their orbitals transform into one another under a four-fold improper rotation about the C–C axis. Waves $\psi_{f,\alpha}$ and $\psi_{f,\beta}$ produced by detachment from ψ_α and ψ_β, respectively, give rise to a two-center description of the free-electron wavefunction $\psi_f = \psi_{f,\alpha} + \psi_{f,\beta}$.

The one-center description of detachment from a monomer unit is given elsewhere [20]. Each of the monomers belongs to the C_{2v} point group and their individual HOMOs are of A_1 symmetry. Under the electric-dipole approximation, $\langle\psi_{f,j}|z|\psi_j\rangle \neq 0$, where z is proportional to the active component of the dipole operator and $j = \alpha, \beta$. The symmetry species of z in the frames of α and β are determined by the orientation of the dimer frame and are given in Fig. 4. For orientation I, only B_2 waves are allowed from α, while β yields waves of B_1 symmetry. For orientation II, both monomer groups yield waves of A_1 symmetry.

Under the s and p approximation, $\psi_{f,\alpha}$ and $\psi_{f,\beta}$ are expanded in the basis of s, p, etc. partial waves emitted from centers α and β, respectively, and all components with $\ell > 1$ are disregarded [20]. For orientation I, this leaves only p waves, as s waves satisfy neither the B_2 nor B_1 restrictions obtained above. Transformed to the LF, the p waves of B_2 (for α) and B_1 (for β) symmetry correspond to the p_z waves sketched in Fig. 4. For orientation II, both s and p waves are allowed, with the p waves limited to p_z components only.

The phase shift between $\psi_{f,\alpha}$ and $\psi_{f,\beta}$ at their respective origins is determined by symmetry and largely unaffected by distance D between the emission centers. This assumption is well justified in the limit of $D \ll \lambda$, where $\lambda = 400$ nm. From symmetry, the overall free-electron wavefunction ψ_f must transform as the dipole component coincident with the laser polarization vector, because ψ_{dimer} is totally symmetric.

For orientation I, the z component of the dipole belongs to the E i.r. of the D_{2d} point group. Hence $\psi_f = \psi_{f,\alpha} + \psi_{f,\beta}$ must be of E symmetry, allowing for both constructive and destructive interference between $\psi_{f,\alpha}$ and $\psi_{f,\beta}$ (combinations I-a and I-b in Fig. 4), as well as for any intermediate phase shift. In addition, the amplitudes of $\psi_{f,\alpha}$ and $\psi_{f,\beta}$ are not constrained to be equal.

In a similar fashion, for orientation II the z dipole component belongs to the B_2 i.r. of the D_{2d} group and the overall wavefunction $\psi_f = \psi_{f,\alpha} + \psi_{f,\beta}$ is of B_2 symmetry. This requirement dictates that the s components of $\psi_{f,\alpha}$ and $\psi_{f,\beta}$ be phase-shifted by π, while the p_z waves contribute with the same sign. In addition, the $\psi_{f,\alpha}$ and $\psi_{f,\beta}$ amplitudes are equal. The relevant s and p waves are sketched in Fig. 4(II-a and II-b).

Thus, the problem of $(CO_2)_2^-$ photodetachment is reduced to interference of s and p waves from two sources. These sources can be thought of as 'centers of mass' of the monomer orbitals and thus separation D between them is in slight excess of the C–C bond length [16]. $D \approx 2$ Å is a reasonable value to use.

For correlation between the dimer and monomer anion photodetachment, we note that the latter is described by the same waves as those emitted from one of the two hypothetical centers in the dual-source model, e.g., center α. The monomer moiety belongs to the C_{2v} point group, in which the dipole operator spans three irreducible representations $A_1 + B_1 + B_2$, yielding three principal orientations with respect to z. In the s and p treatment, each of these orientations yields a p_z wave, in addition to an s wave from the orientation with the A_1 active dipole component [20,26]. The three p_z waves correspond to the α components of the I-a, I-b, and II-b wave pairs (Fig. 4), while the s wave is the α component of II-a.

To compare the monomer and dimer anion PADs, one needs to examine the effect of interference of waves emitted from α and β. The key to the outcome is the de Broglie wavelength λ_e of the emitted electrons. In the energy range characteristic of these measurements, λ_e by far exceeds D. For example, the mid range in Fig. 3 corresponds to 0.7 eV and $\lambda_e = 15$ Å. On this scale, the wave sources α and β separated by $D \approx 2$ Å appear almost overlapped. For a zero initial phase-shift, the overall wave from the dimer anion will appear similar to that from just one source (a monomer), yielding a similar PAD. In the case of opposite phases, the overall wave structure will be different from the monomer-emitted wave, but the corresponding contributions are minimized by destructive interference. Thus, the waves emitted with similar phases contribute the most to the dimer-anion PAD.

In summary, preferential electron ejection along the laser polarization axis occurs for both monomer and dimer anions, independent of their LF orientation. Moreover, the dimer-emitted waves tend to be qualitatively similar to those originating

from the monomer anions, resulting in the similar PADs observed for the monomer and dimer based $(CO_2)_n^-$.

The question then arises: what makes the PAD from $(CS_2)_2^-$ so different from that from CS_2^-?

As was already noted, the covalent dimer anions of CO_2 and CS_2 have different electron configurations. Contrary to $(CO_2)_2^-$, the excess electron in $(CS_2)_2^-$ occupies a vacant orbital of a (hypothetical) neutral species whose electron configuration is doubly excited compared to that of a $(CS_2)_2$ van der Waals dimer [12,17]. Although ambiguity exists as to the electronic symmetry of the $(CS_2)_2^-$ ground state ($^2b_1$ or $^2b_2$) [6,17,18], it is not directly relevant to the present work. Important are the following: (i) the electronic structure of covalent $(CS_2)_2^-$ is not directly related to that of CS_2^-; (ii) the $(CS_2)_2^-$ HOMO (b_1 or b_2) cannot be described in the spirit of Eq. (1) as a superposition of the a_1 HOMOs of two CS_2^- monomers. Thus, the different PADs obtained in the detachment of CS_2^- and covalent $(CS_2)_2^-$ should be expected.

The LCMO approximation can still be used to describe the $(CS_2)_2^-$ HOMO in terms of superposition of two monomer-anion orbitals *other than their HOMOs*. If we assume that the $(CS_2)_2^-$ HOMO is of B_2 symmetry, it can be viewed as a superposition of the b_2 (HOMO–1) orbitals of two CS_2^- monomers. Following the dual-source s and p formalism outlined above, we will conclude that the PAD in the $(CS_2)_2^-$ HOMO detachment should be compared to that from the b_2 (HOMO–1) orbital of CS_2^-. The latter corresponds to the second detachment transition in CS_2^- yielding CS_2 in the a^3B_2 state. This transition was imaged previously (at 267 nm) [20], and indeed its PAD (at a comparable energy) is similar to that for $(CS_2)_2^-$: $\beta = -0.24$ for the b_2^{-1} transition in CS_2^- versus $\beta = -0.17$ for the HOMO detachment in covalent $(CS_2)_2^-$.

5. Summary

Photoelectron images reveal dissimilar lowest-energy detachment transitions in CS_2^- and covalent $(CS_2)_2^-$, yet the PADs in detachment from the monomer and dimer anion cores of $(CO_2)_n^-$ clusters are surprisingly similar. These results are a consequence of distinct electronic–structural properties of $(CS_2)_2^-$ and $(CO_2)_2^-$. In the LCMO representation, the $(CO_2)_2^-$ HOMO is comprised of two monomer-anion HOMOs, while the $(CS_2)_2^-$ HOMO is of different nature, involving lower-lying orbitals of the monomer anion.

Acknowledgements

This work is supported by the NSF Grant No. CHE-0134631, the Beckman Young Investigator Award, and the Packard Fellowship for Science and Engineering.

References

[1] D.W. Chandler, P.L. Houston, J. Chem. Phys. 87 (1987) 1445.
[2] K.M. Ervin, W.C. Lineberger, in: N.G. Adams, L.M. Babcock (Eds.), Advances in Gas Phase Ion Chemistry, vol. 1, JAI Press, Greenwich, 1992, p. 121.
[3] T. Suzuki, B.J. Whitaker, Int. Rev. Phys. Chem. 20 (2001) 313.
[4] K.L. Reid, Ann. Rev. Phys. Chem. 54 (2003) 397.
[5] A.W. Castleman, K.H. Bowen, J. Phys. Chem. 100 (1996) 12911.
[6] T. Maeyama, T. Oikawa, T. Tsumura, N. Mikami, J. Chem. Phys. 108 (1998) 1368.
[7] H. Chen, R.B. Huang, X. Lu, Z.C. Tang, X. Xu, L.S. Zheng, J. Chem. Phys. 112 (2000) 9310.
[8] M. Knapp, O. Echt, D. Kreisle, T.D. Mark, E. Recknagel, Chem. Phys. Lett. 126 (1986) 225.
[9] M.L. Alexander, M.A. Johnson, N.E. Levinger, W.C. Lineberger, Phys. Rev. Lett. 57 (1986) 976.
[10] K.H. Bowen, J.G. Eaton, in: R. Naaman, Z. Vager (Eds.), The Structure of Small Molecules and Ions, Plenum, New York, 1988, p. 147.
[11] M.J. DeLuca, B. Niu, M.A. Johnson, J. Chem. Phys. 88 (1988) 5857.
[12] A. Sanov, S. Nandi, K.D. Jordan, W.C. Lineberger, J. Chem. Phys. 109 (1998) 1264.
[13] E. Surber, A. Sanov, Phys. Rev. Lett. 90 (2003) 093001.
[14] E. Surber, A. Sanov, J. Chem. Phys. 118 (2003) 9192.
[15] R. Mabbs, E. Surber, A. Sanov, Analyst 128 (2003) 765.
[16] S.H. Fleischman, K.D. Jordan, J. Phys. Chem. 91 (1987) 1300.
[17] A. Sanov, W.C. Lineberger, K.D. Jordan, J. Phys. Chem. A 102 (1998) 2509.
[18] T. Tsukuda, T. Hirose, T. Nagata, Chem. Phys. Lett. 279 (1997) 179.

[19] T. Tsukuda, M.A. Johnson, T. Nagata, Chem. Phys. Lett. 268 (1997) 429.
[20] E. Surber, R. Mabbs, A. Sanov, J. Phys. Chem. A 107 (2003) 8215.
[21] M.A. Johnson, W.C. Lineberger, in: J.M. Farrar, W.H. Saunders (Eds.), Techniques for the Study of Ion Molecule Reactions, Wiley, New York, 1988, p. 591.
[22] A.T.J.B. Eppink, D.H. Parker, Rev. Sci. Instr. 68 (1997) 3477.
[23] V. Dribinski, A. Ossadtchi, V.A. Mandelshtam, H. Reisler, Rev. Sci. Instr. 73 (2002) 2634.
[24] J.M. Oakes, G.B. Ellison, Tetrahedron 42 (1986) 6263.
[25] J. Schiedt, R. Weinkauf, Chem. Phys. Lett. 274 (1997) 18.
[26] E. Surber, A. Sanov, J. Chem. Phys. 116 (2002) 5921.